THE JOURNAL OF PHYSICAL CHEMISTRY C

Article

Cite This: J. Phys. Chem. C 2018, 122, 6678−6683

pubs.acs.org/JPCC

Barrierless On-Surface Metal Incorporation in Phthalocyanine-Based Molecules

De-Liang Bao,[†,‡] Yu-Yang Zhang,[†,‡] Shixuan Du,[*,†] Sokrates T. Pantelides,[†,‡] and Hong-Jun Gao[†]

[†]Institute of Physics and University of Chinese Academy of Sciences, Chinese Academy of Sciences, Beijing 100190, China

[‡]Department of Physics and Astronomy and Department of Electrical Engineering and Computer Science, Vanderbilt University, Nashville, Tennessee 37235, United States

Supporting Information

ABSTRACT: On-surface metalation of metal-free phthalocyanine derivatives is a simple and solvent-free way to fabricate MPc compounds. Using phthalocyanine (H_2Pc) molecules on Ag(111) as an example, we investigated the atomic-scale mechanisms of on-surface metalation processes using first-principles calculations based on density functional theory. When the molecules are deposited on a substrate first, we find that transition-metal atoms, except for Zn, drop directly from the vacuum into the molecule's cavity without an energy barrier and bond with the inner four nitrogen atoms, with the two pyrrolic H atoms still in place. Subsequently, the two H atoms transfer to the substrate by overcoming small energy barriers and diffuse away. The substrate participates in the reaction by hybridization. In the alternative process, when metal atoms are adsorbed first on the surface and the H_2Pc molecules are then added, the metal atoms diffuse into the cavity of the molecule via the molecule−surface interface by overcoming finite energy barriers. The above results provide insights into the on-surface metalation that can guide the control of the reaction pathway and products at the atomic level.

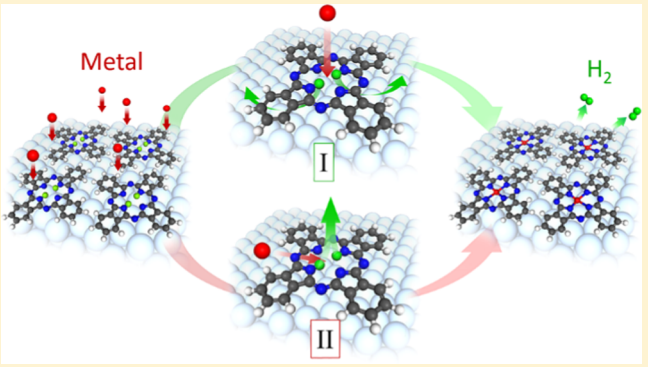

INTRODUCTION

Metal phthalocyanine (MPc) and metal porphyrin (MP) have been synthesized and used as building blocks and functional units for various nanoscale applications,[1] such as chemosensors,[2] active nanocatalysts,[3] organic light-emitting diodes,[4] organic solar cells,[5] and biomedical applications.[6,7] Metalation of phthalocyanine (H_2Pc) or porphyrin (H_2P), namely, the incorporation of a metal atom at the center of the H_2Pc or H_2P molecule, is one way to produce MPcs or MPs with novel physical and chemical properties.[8−12] Compared to the conventional synthesis methods that combine certain precursors under specific conditions,[13] the in situ on-surface metalation has advantages such as mild conditions[14,15] and high yield.[16] Moreover, in situ on-surface metalation of H_2Pc, H_2P, and their derivatives is a superior technique toward the realization of low-dimensional functionalized materials of organometallic compounds.[17−22]

A dozen metal species have so far been reported to be suitable for the metalation reaction of H_2Pc, H_2P, and their derivatives.[11,23−26] Although there have been many experimental investigations of metalation in solvents and on substrates, only a few such works focus on the mechanism of the metalation process of H_2P.[27,28] Buchner et al. found that the metalation reaction occurs rapidly at room temperature by depositing Fe atoms onto preadsorbed tetraphenylporphyrin (H_2TPP) monolayer on Ag(111), whereas additional annealing is needed when post-depositing H_2TPP molecules onto predeposited Fe atoms on the surface.[29] These findings indicate that there are different reaction paths for the metalation reactions. Kretschmann et al. used X-ray photoelectron spectroscopy to investigate porphyrin metalation by Zn and detected an intermediate state, in which the metal atom bonds to the molecule's N atoms, whereas the pyrrolic H atoms remain in place, the so-called "sitting atop complexes" (SAT).[30]

Theoretical investigations of the metalation processes of H_2Pc and H_2P have so far been limited to the gas phase. In particular, Shubina et al. calculated the dehydrogenation energy barrier of freestanding SAT complexes, i.e., the barrier for a porphyrin molecule with a single metal atom on top to transform to a metal porphyrin molecule and a free H_2 molecule.[27] When metalation occurs on a substrate, however, substrate-induced phenomena have been observed. For example, it has been found that the metalation temperature is higher when metal atoms are deposited on the substrate before the deposition of porphyrins.[29] Considering the potential applications of MPc-based two-dimensional materials, understanding the mechanism of the on-surface metalation process, including the effect of the substrate, would be useful for both

Received: January 3, 2018
Revised: March 1, 2018
Published: March 6, 2018

DOI: 10.1021/acs.jpcc.8b00086
J. Phys. Chem. C 2018, 122, 6678−6683

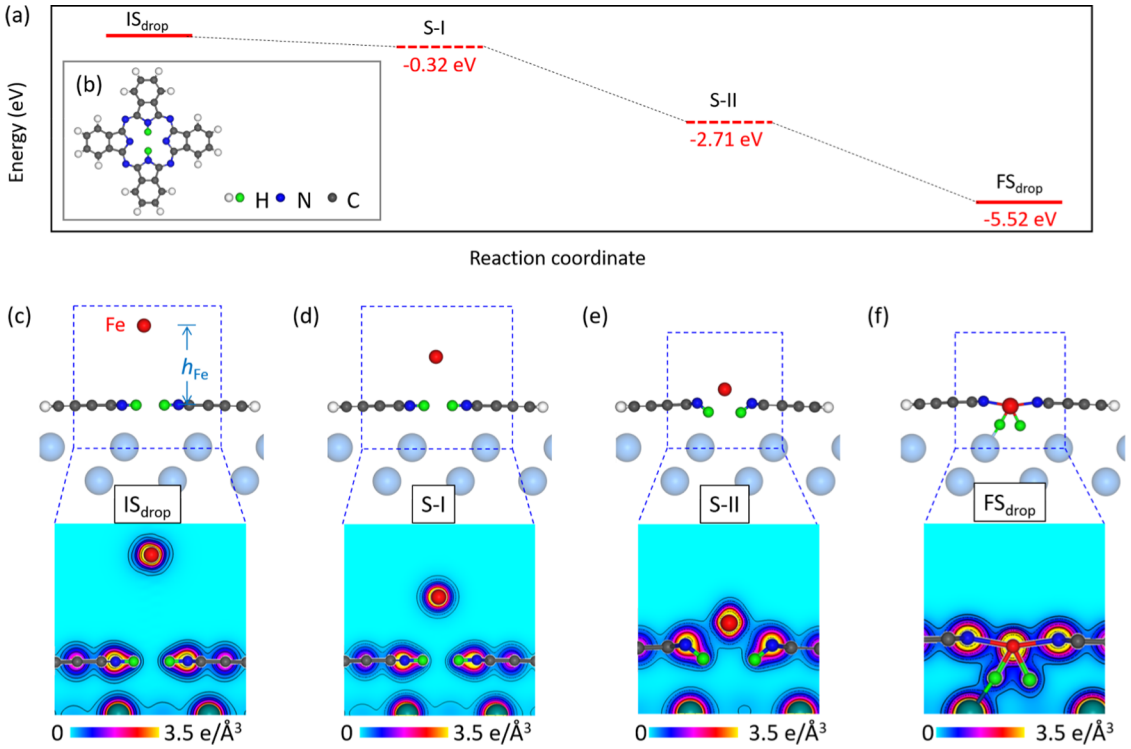

Figure 1. Dropping-down reaction pathway for the metalation of a H_2Pc molecule on a Ag(111) surface using an Fe atom. (a) Energy profile of the dropping-down process. Each step corresponds to the structures shown in the upper panels in (c). (b) Top view of a H_2Pc molecule. (c–f) Upper panels: cross sections of the atomic configurations of the initial state (IS_{drop}), S-I, S-II, and the final state (FS_{drop}) shown in (a), respectively. Lower panels: cross sections of the electronic densities of the IS_{drop}, S-I, S-II, and the FS_{drop} with a zoomed-in scale marked by the blue dashed box in the upper panels. The cross sections are crossing the Fe atom and the two inner H atoms. The contour lines in the lower panels in (c)–(f) indicate the electron density ranges from 0.54 to 3.0 e/Å^3, with intervals of 0.4 e/Å^3.

the synthesis of metal–organic molecules and the functionalization of two-dimensional organic frameworks using metals.

In this study, we use quantum mechanical calculations based on density functional theory (DFT) to investigate the on-surface metalation process of phthalocyanine-based molecules, using H_2Pc molecules adsorbed on a Ag(111) surface as a prototype system. In the process, when metal atoms are added onto preadsorbed H_2Pc molecules on a Ag(111) surface, we find that transition-metal atoms drop directly into the cavities of molecules without an energy barrier, whereas a closed-shell Zn atom exhibits a finite energy barrier of 0.86 eV. All investigated metal atoms first form an intermediate SAT complex, in which the two pyrrolic hydrogen atoms still bond to the molecule, whereas one of the two H atoms also bonds to a substrate atom. Subsequently, the two pyrrolic H atoms break off the metal-Pc (MPc) complex and bond to the substrate, overcoming a small barrier, 0.4 eV in the case of Fe, and then diffuse away underneath the MPc molecule. By analyzing the electron density redistribution during the metalation process, we find that the two pyrrolic H atoms bond to both the substrate and the Fe atom in the SAT intermediate state. For the alternative process, when the metal atoms are deposited on the surface first, the metal atoms must diffuse through the H_2Pc/substrate interface into the central cavity of the H_2Pc molecules, overcoming a finite energy barrier. This result is consistent with the observations that an annealing step is needed to complete the metalation process.[29]

COMPUTATIONAL DETAILS

First-principles calculations based on density functional theory (DFT) were performed in a plane-wave formulation with the projector augmented wave method, as implemented in the Vienna ab initio simulation package.[31,32] The Perdew–Burke–Ernzernhof[33] parameterization of the generalized gradient approximation[34] was used. Grimme's empirical correction scheme was also used to take the van der Waals interaction into account.[35] The cutoff energy of the plane waves was 400 eV. The Brillouin zone was sampled with Γ-point in all calculations. Four-layer atomic slabs were used to simulate the Ag(111) substrate, with molecules and Fe atoms adsorbed on one side. The vacuum layer is 25 Å between neighboring slabs. In structural relaxations, two bottom layers of Ag atoms were fixed, whereas the upper two layers of Ag atoms and the molecules were totally relaxed until the force on every atom was smaller than 0.02 eV/Å. The reaction path of the metalation was modeled by the climbing image nudged elastic band method.[36,37]

RESULTS AND DISCUSSION

H_2Pc is a macrocyclic aromatic molecule with a central cavity, in which the two hydrogen atoms (shown as green balls in the inset of Figure 1a, marked as Figure 1b) can be replaced by various metal atoms. We will use Fe atoms as a prototype example for a detailed investigation of the on-surface metalation because Fe is widely used with phthalocyanine derivatives both in the life sciences and for surface functionalization. We first investigate the case when the H_2Pc molecules are deposited

DOI: 10.1021/acs.jpcc.8b00086
J. Phys. Chem. C 2018, 122, 6678–6683

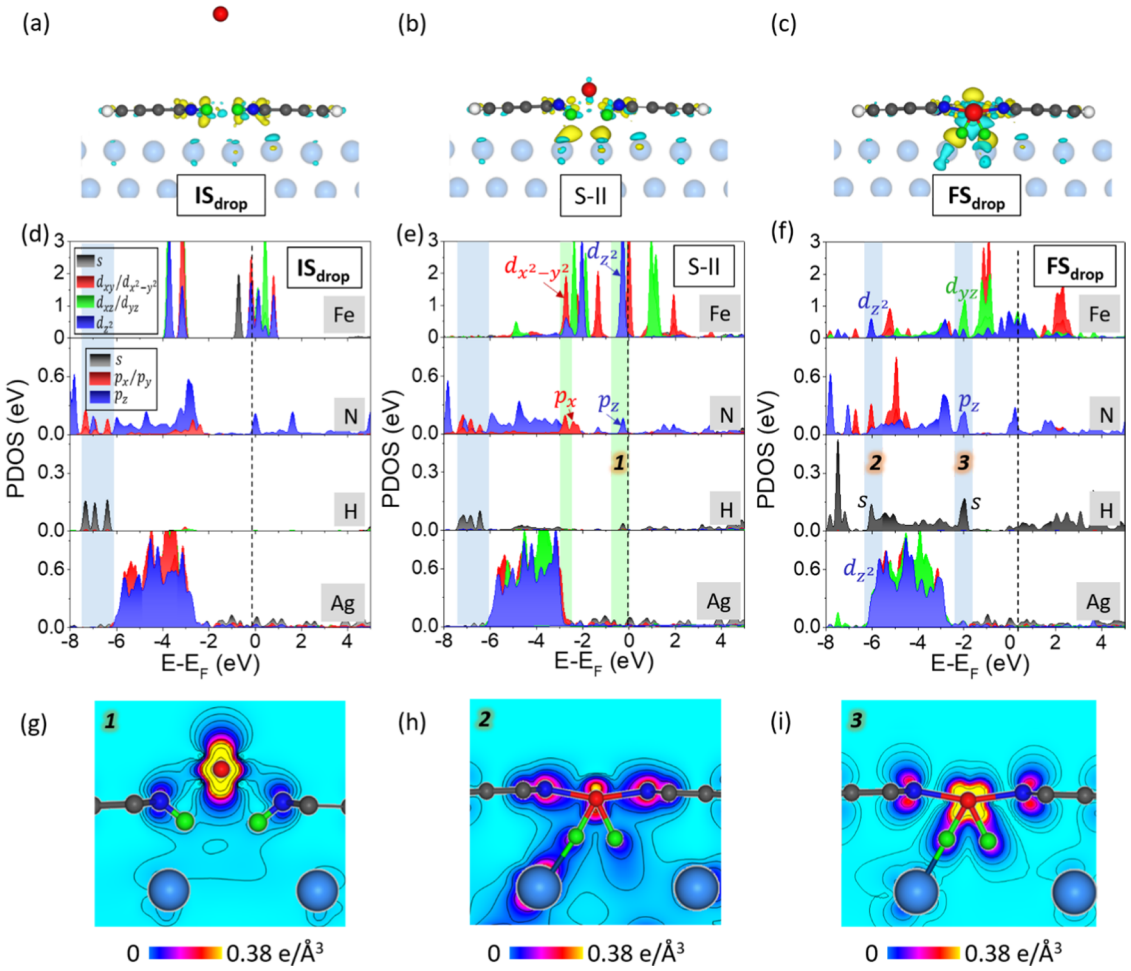

Figure 2. Electronic properties of the IS_{drop}, S-II, and FS_{drop} in the metalation process shown in Figure 1. (a–c) Side views of the electron density difference for IS_{drop}, S-II, and FS_{drop}, respectively. The yellow areas represent electron accumulation, and the blue areas represent electron depletion. The isosurface is ~0.01 e/Å^3. (d–f) Projected density of states (PDOSs) on Fe, pyrrolic N, pyrrolic H, and Ag atoms close to pyrrolic H atoms for the IS_{drop}, S-II, and FS_{drop}, respectively. (g–i) Zoomed-in cross sections of the electronic densities within the energy ranges marked as 1, 2, and 3 in (e) and (f) (note that both (h) and (i) correspond to the configuration shown in (c) and that (g) corresponds to the configuration shown in (b)).

first on a Ag(111) substrate and the metal atoms are then added.

From Figure 1c–f, one can see the configuration and electronic density evolution during the dropping-down path of Fe from vacuum into the molecule. The initial state (IS_{drop}) is a combination of a single H_2Pc molecule adsorbed flatly on the Ag(111) surface with a single Fe atom suspended over the central cavity of the H_2Pc molecule. The height (h_{Fe}) of the Fe atom from the H_2Pc molecule is chosen to be about 5.7 Å, where there is no electronic interaction between the metal atom and the molecule. The cross section of the electronic density of the IS_{drop} is shown in the lower panel in Figure 1c. As expected, there is little electronic density (less than 10^{-7} e/Å^3) between the Fe atom and the H_2Pc molecule. As the Fe atom is placed closer to the H_2Pc molecule, the energy is monotonically lower, i.e., the Fe atom moves toward the cavity of the molecule via a barrierless path (Figure 1a). The energy of the final state (FS_{drop}) is 5.52 eV lower than that of the IS_{drop}, implying an exothermic process.

In the FS_{drop} (Figure 1f), the two pyrrolic H atoms (shown as green balls in the models) in the cavity of the molecule are pushed into the molecule–substrate interface, still bond to the Fe atom, and partially bond to the substrate Ag atom (as evinced by the electron density in Figure 1f). The H–Fe bond lengths are 1.54 and 1.59 Å. The H–Ag bond length for the left H atom in Figure 1f is 1.90 Å, and the distances from the right H atom to its nearest Ag atoms are 2.09 and 2.07 Å. Therefore, an SAT configuration is formed. The structural stability of the SAT configuration in Figure 1f is checked by calculating the phonon spectra.[38] There are no negative-frequency phonon modes, which is an indication of the structural stability.

To elucidate the influence of the substrate during the metalation process, the electron density difference profiles of the IS_{drop}, S-II, and FS_{drop} are shown in Figure 2a–c, respectively. The electron density differences are calculated as $\Delta\rho = \rho_{tot} - \rho_{sub} - \rho_{mol}$, where ρ_{tot} is the electron density of the total system, ρ_{sub} is the electron density of the Ag substrate, and ρ_{mol} is the electron density of the Fe–H_2Pc complex.[39] $\Delta\rho$ represents the change of the electron densities between the Fe–H_2Pc complex and the substrate induced by the complex–substrate interactions.

The side views of electron density differences in Figure 2a–c show that electron redistribution occurs at the molecular plane for IS_{drop}, S-II, and FS_{drop}. For FS_{drop}, there is extra redistribution of the electrons on different d orbitals of Fe when Fe bonds with the four pyrrolic nitrogen atoms. When the Fe atom drops down to the central cavity, the electron distribution of the Ag atoms under the two pyrrolic H atoms

DOI: 10.1021/acs.jpcc.8b00086
J. Phys. Chem. C 2018, 122, 6678–6683

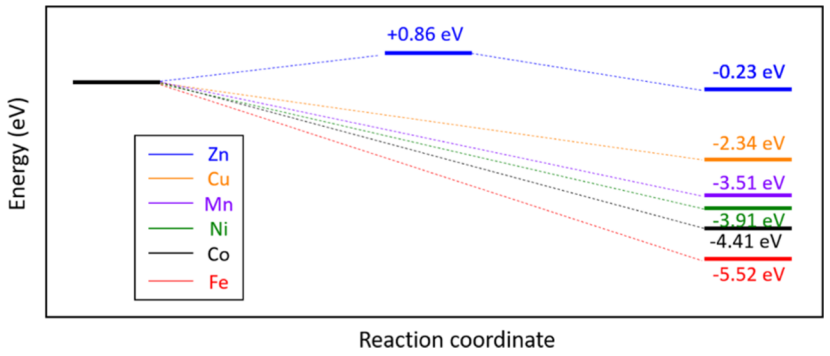

Figure 3. Energy profile of dropping-down path for different transition metals. The numbers represent the energy values related to the initial state.

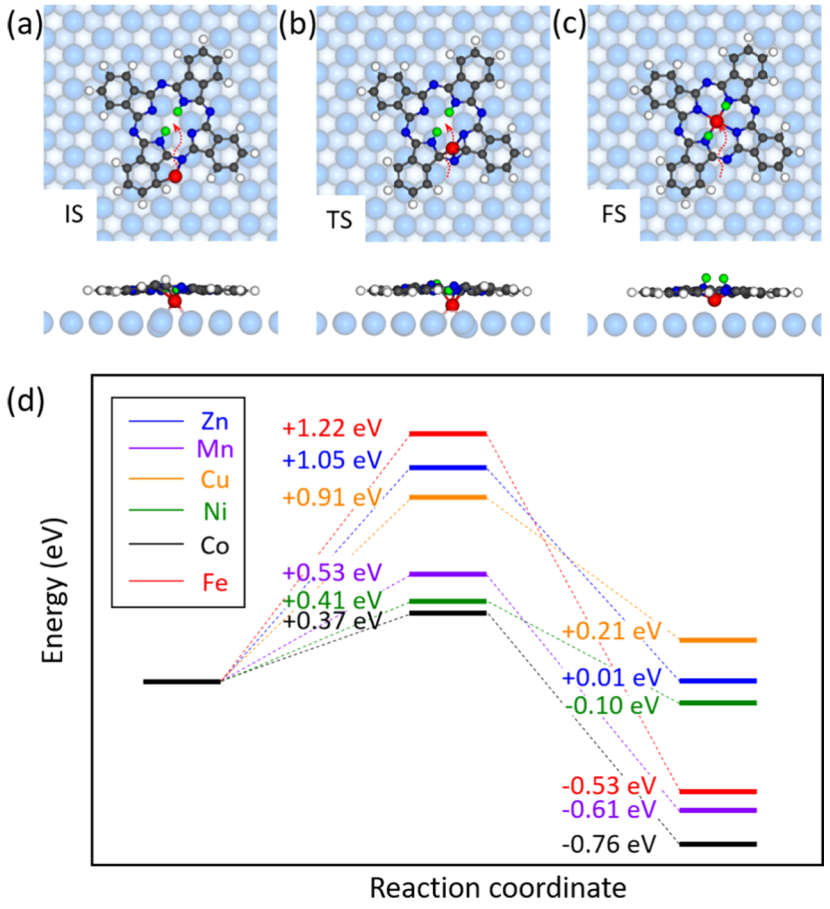

Figure 4. Structures and energy profile of the metalation process via a diffusing-in path. (a–c) Top views and side views of IS_{diff}, transition state (TS_{diff}), and FS_{diff}, respectively. (d) Energy profiles for investigated transition metals via the diffusing-in path.

changes significantly (Figure 2b,c), suggesting a non-negligible attraction of the Ag atoms to the Fe atom.

Comparing the PDOSs of the three states, we found that the bonding states of two pyrrolic H atoms keep unchanged in the IS_{drop} and S-II (see the shadow regions marked with light blue in Figure 2d,e). When the Fe atom is close to the H_2Pc molecule in the S-II, the coupling between Fe and the H_2Pc skeleton comes from the interaction of the out-of-plane d_{z^2} orbital of Fe with the p_z orbitals of N atoms and the interaction of in-plane $d_{x^2-y^2}$ orbital of Fe with in-plane p_x orbital of N atoms (see the shadow regions marked with light green in Figure 2e). The subtle electron accumulation above the substrate in the S-II comes from both the Fe–H_2Pc compound and the substrate due to the effect of the interface, resulting in the enhanced d_{xz}/d_{yz} orbitals of the Ag atom. For the FS_{drop}, the bonding state of two pyrrolic H changes significantly due to the occupation of Fe at the center of the Pc skeleton and the downshift of the two pyrrolic H atoms. The two H atoms bond to both the Ag substrate and the Fe atom, as shown in the shadow region marked with light blue in Figure 2f. The zoomed-in cross sections of the electronic densities within the energy ranges marked as 1, 2, and 3 in Figure 2e,f are shown in Figure 2g–i. The Ag substrate attracts and stabilizes the two pyrrolic H atoms when Fe approaches the Pc skeleton, resulting in a barrierless process. From Figure S2, we found that the PDOS of pyrrolic N atoms in the FS_{drop} is the same as that of iron phthalocyanine (FePc)/Ag, indicating that the Fe successfully coordinates at the center of H_2Pc. The PDOS of

DOI: 10.1021/acs.jpcc.8b00086
J. Phys. Chem. C 2018, 122, 6678–6683

Fe in the FS_{drop} is still different from that in FePc/Ag due to the two pyrrolic H atoms underneath.

Several transition metals have been investigated in the dropping-down reaction pathway. The energy profiles are shown in Figure 3. All of the transition-metal atoms we investigated, namely, Cu, Mn, Ni, Co, and Fe, follow the barrierless coordination process discussed above. The element Zn, on the other hand, exhibits a 0.86 eV energy barrier, most likely because its 3d and 4s orbitals are fully occupied, which makes it less prone to interact and hybridize. Each of the FS_{drop} for the investigated transition-metal atoms has a similar configuration to the one shown in Figure 2c. The energy differences between FS_{drop} and IS_{drop} are 0.23, 2.34, 3.51, 3.91, and 4.41 eV for Zn, Cu, Mn, Ni, and Co, respectively, indicating exothermic processes.

To produce a pure FePc molecule on surface, in the SAT state, detachment of H atoms from Fe is necessary. In the following, we report the energy barriers of the detachment of H atoms from the transition-metal atoms. Calculation results (Figure S1) show that the dehydrogenation processes of all metal species are stepwise, detaching one hydrogen atom first and then the other. The two-step process is caused by the substrate and is different from what happens in the gas phase, where the H atoms first combine together and then release as a H_2 molecule.[27] For the transition metals we investigated, the barriers of dehydrogenating the first/second H atom for Fe, Mn, Zn, Ni, and Co are 0.1/0.4, 0.0/0.0, 0.26/0.32, 0.23/0.35, and 0.0/0.14 eV, respectively. The barriers are comparable and generally somewhat lower than the published gas-phase calculation results, which are 0.0, 1.51, 1.27, and 0.68 eV for Fe, Zn, Ni, and Co, respectively.[27] Moreover, the barriers are small enough to be overcome at room temperature.

Subsequently, taking FePc-H_2/Ag(111) as an example, when the released H atoms diffuse away from the FePc/Ag interface overcoming a finite barrier, 0.12 eV, the energy of the system decreases by 1.33 eV, indicating a process that can easily happen at room temperature.

The alternative approach to metalation, namely, depositing the metal atoms on the surface first and then adding the molecules, has also been investigated. Taking the H_2Pc molecule as an adsorbate on a substrate, a metal atom first adsorbs on the substrate, migrates close to a H_2Pc molecule (IS_{diff}, shown in Figure 4a), and then diffuses into the molecule's central cavity (transition state, TS_{diff}, shown in Figure 4b). Subsequently, the metal atom bonds to the pyrrolic N atoms in the cavity by pushing the two central H atoms upward (FS_{diff}, shown in Figure 4c). From the energy profiles in Figure 4d, one can see that the investigated transition metals must overcome energy barriers of 1.22, 1.05, 0.91, 0.54, 0.53, and 0.41 eV for Fe, Zn, Cu, Co, Mn, and Ni, respectively. These results indicate higher reaction barriers in comparison with the dropping-down path. Taking the Ni-H_2Pc/Ag(111) as an example, our calculations show that the dehydrogenation barrier during the diffusing-in path is 0.84 eV, which is comparable to the result in the gas-phase calculations (1.27 eV)[27] in 2007. In both cases, the two H atoms form a H_2 molecule, which desorbs. The higher barriers mentioned above are consistent with the experimental finding that an annealing step is needed to complete the metalation process in this approach.[30]

CONCLUSIONS

In conclusion, we investigated the atomic-scale mechanisms for two different on-surface metalation processes of phthalocyanine-based molecules. In the case when H_2Pc molecules are adsorbed on a Ag(111) surface first, a barrierless metalation process is found for transition-metal atoms, but not for the closed-shell Zn atom. The dropping-down path, corresponding to the metal atoms dropping down to the molecular cavities from the vacuum above, is demonstrated to be the energetically favored mechanism for the on-surface metalation. The role of the substrate is both to supply a platform for molecules to be adsorbed as well as to influence the reaction electronically. Metalation through the alternative process, when the metal atoms are deposited on the surface first, entails relatively large energy barriers, which requires an annealing step, as observed. This work provides insights into the on-surface metalation reaction design and construction of low-dimensional functionalized materials with organometallic compounds by surface-mediated reactions.

ASSOCIATED CONTENT

Supporting Information

The Supporting Information is available free of charge on the ACS Publications website at DOI: 10.1021/acs.jpcc.8b00086.

Stepwise transfer process of the H atoms from transition-metal atoms to the substrate through dropping-down path; projected density of states (PDOSs) of the State-II and FS_{drop} in the dropping-down path (PDF)

AUTHOR INFORMATION

Corresponding Author

*E-mail: sxdu@iphy.ac.cn.

ORCID

De-Liang Bao: 0000-0002-5070-4765
Yu-Yang Zhang: 0000-0002-9548-0021
Shixuan Du: 0000-0001-9323-1307
Hong-Jun Gao: 0000-0002-6766-0623

Notes

The authors declare no competing financial interest.

ACKNOWLEDGMENTS

The authors thank Professor Werner A. Hofer and Professor Min Ouyang for constructive discussions and suggestions. They acknowledge the financial support from the National Basic Research Program of China (2013CBA01600), the National Natural Science Foundation of China (Nos. 61390501, 61471337, 61622116, and 51325204), National Key Scientific Instrument and Equipment Development Project of China (No. 2013YQ1203451), the CAS Pioneer Hundred Talents Program, and the Transregional Collaborative Research Center TRR 61 (21661132006). Work at Vanderbilt (S.T.P., D.-L.B.) was supported by the McMinn Endowment. Computations by Y.-Y.Z. were carried out at the National Energy Research Scientific Computing Center, a DOE Office of Science User Facility supported by the Office of Science of the U.S. Department of Energy under Contract No. DE-AC02-05CH11231. A portion of the research was performed in the CAS Key Laboratory of Vacuum Physics. Work at Vanderbilt was supported by the McMinn Endowment.

DOI: 10.1021/acs.jpcc.8b00086
J. Phys. Chem. C 2018, 122, 6678−6683

REFERENCES

(1) Elemans, J. A. A. W.; van Hameren, R.; Nolte, R. J. M.; Rowan, A. E. Molecular Materials by Self-Assembly of Porphyrins, Phthalocyanines, and Perylenes. *Adv. Mater.* **2006**, *18*, 1251−1266.

(2) Rakow, N. A.; Suslick, K. S. A Colorimetric Sensor Array for Odour Visualization. *Nature* **2000**, *406*, 710−713.

(3) Sedona, F.; Di Marino, M.; Forrer, D.; Vittadini, A.; Casarin, M.; Cossaro, A.; Floreano, L.; Verdini, A.; Sambi, M. Tuning the Catalytic Activity of Ag(110)-Supported Fe Phthalocyanine in the Oxygen Reduction Reaction. *Nat. Mater.* **2012**, *11*, 970−977.

(4) Endo, A.; Ogasawara, M.; Takahashi, A.; Yokoyama, D.; Kato, Y.; Adachi, C. Thermally Activated Delayed Fluorescence from Sn^{4+}−Porphyrin Complexes and Their Application to Organic Light Emitting Diodes—a Novel Mechanism for Electroluminescence. *Adv. Mater.* **2009**, *21*, 4802−4806.

(5) Yella, A.; Lee, H.-W.; Tsao, H. N.; Yi, C.; Chandiran, A. K.; Nazeeruddin, M. K.; Diau, E. W.-G.; Yeh, C.-Y.; Zakeeruddin, S. M.; Grätzel, M. Porphyrin-Sensitized Solar Cells with Cobalt (Ii/Iii)−Based Redox Electrolyte Exceed 12 Percent Efficiency. *Science* **2011**, *334*, 629−634.

(6) Figueira, F.; Pereira, P. M. R.; Silva, S.; Cavaleiro, J. A. S.; Tome, J. Porphyrins and Phthalocyanines Decorated with Dendrimers: Synthesis and Biomedical Applications. *Curr. Org. Chem.* **2014**, *11*, 110−126.

(7) Sun, R. W.-Y.; Che, C.-M. The Anti-Cancer Properties of Gold (Iii) Compounds with Dianionic Porphyrin and Tetradentate Ligands. *Coord. Chem. Rev.* **2009**, *253*, 1682−1691.

(8) Cochran, A. G.; Schultz, P. G. Antibody-Catalyzed Porphyrin Metallation. *Science* **1990**, *249*, 781−783.

(9) Diller, K.; Papageorgiou, A. C.; Klappenberger, F.; Allegretti, F.; Barth, J. V.; Auwärter, W. In Vacuo Interfacial Tetrapyrrole Metallation. *Chem. Soc. Rev.* **2016**, *45*, 1629−1656.

(10) Hiroto, S.; Miyake, Y.; Shinokubo, H. Synthesis and Functionalization of Porphyrins through Organometallic Methodologies. *Chem. Rev.* **2017**, *117*, 2910−3043.

(11) Gottfried, J. M. Surface Chemistry of Porphyrins and Phthalocyanines. *Surf. Sci. Rep.* **2015**, *70*, 259−379.

(12) Yan, L.-H.; et al. Adsorption Behavior of Fe Atoms on a Naphthalocyanine Monolayer on Ag(111) Surface. *Chin. Phys. B* **2015**, *24*, No. 076802.

(13) Sakamoto, K.; Ohno-Okumura, E. Syntheses and Functional Properties of Phthalocyanines. *Materials* **2009**, *2*, 1127−1180.

(14) Nowakowski, J.; Wackerlin, C.; Girovsky, J.; Siewert, D.; Jung, T. A.; Ballav, N. Porphyrin Metalation Providing an Example of a Redox Reaction Facilitated by a Surface Reconstruction. *Chem. Commun.* **2013**, *49*, 2347−2349.

(15) Zhou, H.; Liu, J.; Du, S.; Zhang, L.; Li, G.; Zhang, Y.; Tang, B. Z.; Gao, H.-J. Direct Visualization of Surface-Assisted Two-Dimensional Diyne Polycyclotrimerization. *J. Am. Chem. Soc.* **2014**, *136*, 5567−5570.

(16) Marbach, H. Surface-Mediated in Situ metalation of Porphyrins at the Solid−Vacuum Interface. *Acc. Chem. Res.* **2015**, *48*, 2649−2658.

(17) Gottfried, J. M.; Flechtner, K.; Kretschmann, A.; Lukasczyk, T.; Steinrück, H.-P. Direct Synthesis of a Metalloporphyrin Complex on a Surface. *J. Am. Chem. Soc.* **2006**, *128*, 5644−5645.

(18) Auwärter, W.; Weber-Bargioni, A.; Brink, S.; Riemann, A.; Schiffrin, A.; Ruben, M.; Barth, J. V. Controlled Metalation of Self-Assembled Porphyrin Nanoarrays in Two Dimensions. *ChemPhysChem* **2007**, *8*, 250−254.

(19) Goldoni, A.; Pignedoli, C. A.; Santo, G. D.; Castellarin-Cudia, C.; Magnano, E.; Bondino, F.; Verdini, A.; Passerone, D. Room Temperature Metalation of 2h-Tpp Monolayer on Iron and Nickel Surfaces by Picking up Substrate Metal Atoms. *ACS Nano* **2012**, *6*, 10800−10807.

(20) Wang, J.; Zhong, Y.; Wang, L.; Zhang, N.; Cao, R.; Bian, K.; Alarid, L.; Haddad, R. E.; Bai, F.; Fan, H. Morphology-Controlled Synthesis and Metalation of Porphyrin Nanoparticles with Enhanced Photocatalytic Performance. *Nano Lett.* **2016**, *16*, 6523−6528.

(21) Wu, R.; Yan, L.; Zhang, Y.; Ren, J.; Bao, D.; Zhang, H.; Wang, Y.; Du, S.; Huan, Q.; Gao, H.-J. Self-Assembled Patterns and Young's Modulus of Single-Layer Naphthalocyanine Molecules on Ag(111). *J. Phys. Chem. C* **2015**, *119*, 8208−8212.

(22) Liu, L.; et al. Revealing the Atomic Site-Dependent g Factor within a Single Magnetic Molecule Via the Extended Kondo Effect. *Phys. Rev. Lett.* **2015**, *114*, No. 126601.

(23) Wang, C.; Fan, Q.; Hu, S.; Ju, H.; Feng, X.; Han, Y.; Pan, H.; Zhu, J.; Gottfried, J. M. Coordination Reaction between Tetraphenylporphyrin and Nickel on a Tio_2(110) Surface. *Chem. Commun.* **2014**, *50*, 8291−8294.

(24) Ditze, S.; Stark, M.; Drost, M.; Buchner, F.; Steinrück, H. P.; Marbach, H. Activation Energy for the Self-Metalation Reaction of 2h-Tetraphenylporphyrin on Cu(111). *Angew. Chem., Int. Ed.* **2012**, *51*, 10898−10901.

(25) Sperl, A.; Kröger, J.; Berndt, R. Controlled Metalation of a Single Adsorbed Phthalocyanine. *Angew. Chem., Int. Ed.* **2011**, *50*, 5294−5297.

(26) Weber-Bargioni, A.; Reichert, J.; Seitsonen, A. P.; Auwarter, W.; Schiffrin, A.; Barth, J. V. Interaction of Cerium Atoms with Surface-Anchored Porphyrin Molecules. *J. Phys. Chem. C* **2008**, *112*, 3453−3455.

(27) Shubina, T. E.; Marbach, H.; Flechtner, K.; Kretschmann, A.; Jux, N.; Buchner, F.; Steinrück, H.-P.; Timothy, Clark; Gottfried, J. M. Principle and Mechanism of Direct Porphyrin Metalation: Joint Experimental and Theoretical Investigation. *J. Am. Chem. Soc.* **2007**, *129*, 9476−9483.

(28) Röckert, M.; et al. Insights in Reaction Mechanistics: Isotopic Exchange During the Metalation of Deuterated Tetraphenyl-21,23d-Porphyrin on Cu(111). *J. Phys. Chem. C* **2014**, *118*, 26729−26736.

(29) Buchner, F.; Flechtner, K.; Bai, Y.; Zillner, E.; Kellner, I.; Steinrück, H.-P.; Marbach, H.; Gottfried, J. M. Coordination of Iron Atoms by Tetraphenylporphyrin Monolayers and Multilayers on Ag(111) and Formation of Iron-Tetraphenylporphyrin. *J. Phys. Chem. C* **2008**, *112*, 15458−15465.

(30) Kretschmann, A.; Walz, M.-M.; Flechtner, K.; Steinrück, H.-P.; Gottfried, J. M. Tetraphenylporphyrin Picks up Zinc Atoms from a Silver Surface. *Chem. Commun.* **2007**, 568−570.

(31) Vanderbilt, D. Soft Self-Consistent Pseudopotentials in a Generalized Eigenvalue Formalism. *Phys. Rev. B* **1990**, *41*, 7892−7895.

(32) Kresse, G.; Furthmüller, J. Efficient Iterative Schemes for Ab Initio Total-Energy Calculations Using a Plane-Wave Basis Set. *Phys. Rev. B* **1996**, *54*, 11169−11186.

(33) Perdew, J. P.; Burke, K.; Ernzerhof, M. Generalized Gradient Approximation Made Simple. *Phys. Rev. Lett.* **1996**, *77*, 3865−3868.

(34) Perdew, J. P.; Chevary, J. A.; Vosko, S. H.; Jackson, K. A.; Pederson, M. R.; Singh, D. J.; Fiolhais, C. Atoms, Molecules, Solids, and Surfaces: Applications of the Generalized Gradient Approximation for Exchange and Correlation. *Phys. Rev. B* **1992**, *46*, 6671−6687.

(35) Wu, X.; Vargas, M. C.; Nayak, S.; Lotrich, V.; Scoles, G. Towards Extending the Applicability of Density Functional Theory to Weakly Bound Systems. *J. Chem. Phys.* **2001**, *115*, 8748−8757.

(36) Henkelman, G.; Uberuaga, B. P.; Jónsson, H. A Climbing Image Nudged Elastic Band Method for Finding Saddle Points and Minimum Energy Paths. *J. Chem. Phys.* **2000**, *113*, 9901−9904.

(37) Henkelman, G.; Jónsson, H. Improved Tangent Estimate in the Nudged Elastic Band Method for Finding Minimum Energy Paths and Saddle Points. *J. Chem. Phys.* **2000**, *113*, 9978−9985.

(38) Zhang, Y. Y.; Mishra, R.; Pennycook, T. J.; Borisevich, A. Y.; Pennycook, S. J.; Pantelides, S. T. Oxygen Disorder, a Way to Accommodate Large Epitaxial Strains in Oxides. *Adv. Mater. Interfaces* **2015**, *2*, No. 1500344.

(39) Zhang, Y. Y.; Du, S. X.; Gao, H.-J. Binding Configuration, Electronic Structure, and Magnetic Properties of Metal Phthalocyanines on a Au(111) Surface Studied with Ab Initio calculations. *Phys. Rev. B* **2011**, *84*, No. 125446.

DOI: 10.1021/acs.jpcc.8b00086
J. Phys. Chem. C 2018, 122, 6678−6683